Verticillium dahliae disease resistance and the regulatory pathway for maturity and tuberization in potato

Tai, Helen H.; De Koyer, David ; Sønderkær, Mads; Hedegaard, Sanne; Lague, Martin ; Goyer, Claudia; Nolan, Lana; Davidson, Charlotte ; Gardner, Kyle; Neilson, Jonathan ; Paudel, Jamuna Risal; Murphy, Agnes; Bizimungu, Benoit; Wang, Hui Ying; Xiong, Xingyao; Halterman, Dennis; Nielsen, Kåre Lehmann

Published in:
The Plant Genome

DOI (link to publication from Publisher):
10.3835/plantgenome2017.05.0040

Publication date:
2018

Document Version
Publisher's PDF, also known as Version of record

Published online January 4, 2018

Verticillium dahliae Disease Resistance and the Regulatory Pathway for Maturity and Tuberization in Potato

Helen H. Tai,* David De Koeyer, Mads Sønderkær, Sanne Hedegaard, Martin Lagüe, Claudia Goyer, Lana Nolan, Charlotte Davidson, Kyle Gardner, Jonathan Neilson, Jamuna Risal Paudel, Agnes Murphy, Benoit Bizimungu, Hui Ying Wang, Xingyao Xiong, Dennis Halterman, and Kåre Lehmann Nielsen

ABSTRACT

Verticillium dahliae Kleb. is a pathogenic fungus causing wilting, chlorosis, and early dying in potato (*Solanum tuberosum* L.). Genetic mapping of resistance to *V. dahliae* was done using a diploid population of potato. The major quantitative trait locus (QTL) for *Verticillium* resistance was found on chromosome 5. The *StCDF1* gene, controlling earliness of maturity and tuberization, was mapped within the interval. Another QTL on chromosome 9 co-localized with the *Ve2 Verticillium* wilt resistance gene marker. Epistasis analysis indicated that the loci on chromosomes 5 and 9 had a highly significant interaction, and that *StCDF1* functioned downstream of *Ve2*. The *StCDF1* alleles were sequenced and found to encode StCDF1.1 and StCDF1.3. Interaction between the *Ve2* resistance allele and the *StCDF1.3* was demonstrated, but not for *StCDF1.1*. Genome-wide expression QTL (eQTL) analysis was performed and genes with eQTL at the *StCDF1* and *Ve2* loci were both found to have similar functions involving the chloroplast, including photosynthesis, which declines in both maturity and *Verticillium* wilt. Among the gene ontology (GO) terms that were specific to genes with eQTL at the *Ve2*, but not the *StCDF1* locus, were those associated with fungal defense. These results suggest that *Ve2* controls fungal defense and reduces early dying in *Verticillium* wilt through affecting genetic pathway controlling tuberization timing.

Core Ideas

- Verticillium wilt resistance is linked to control of tuberization in potato.
- The StCDF1 tuberization gene is epistatic to the Ve2 resistance gene.
- eQTL can be used to examine gene networks for complex traits.

Verticillium wilt is caused by fungal colonization of the vascular system in plants (Johnson and Dung, 2010; Pegg and Brady, 2002) and is primarily a problem in temperate regions with decreased incidence in the tropics. *Verticillium dahliae* is the species with the greatest economic impact as a result of its broad

H.H. Tai, D. De Koeyer, M. Lagüe, C. Goyer, L. Nolan, C. Davidson, K. Gardner, J. Neilson, J.R. Paudel, A. Murphy, B. Bizimungu, Agriculture and Agri-Food Canada, Fredericton Research and Development Centre, P.O. Box 20280, Fredericton, New Brunswick, Canada E3B 4Z7; M. Sønderkær, S. Hedegaard, K.L. Nielsen, Dep. of Chemistry and Bioscience, Fredrik Bajers Vej 7, Aalborg Univ., 9220 Aalborg, Denmark; H.Y. Wang, X. Xiong, College of Horticulture and Landscape, Hunan Agriculture Univ., Hunan, Changsha, China 410128; D. Halterman, USDA-ARS, Vegetable Crops Research Unit, Madison, WI 53706; D. De Koeyer, International Institute of Tropical Agriculture, PMB 5320, Oyo Road, Ibadan 200001, Oyo State, Nigeria. Received 17 May 2017. Accepted 31 Aug. 2017. *Corresponding author (Helen.Tai@agr.gc.ca).

Abbreviations: CAPS, cleaved amplified polymorphic sequence; CDF, cycling DNA-binding one finger factor; CO, *CONSTANS*; DAP, days after planting; DArT, diversity array technology; DeepSAGE, deep serial analysis of gene expression; DOF, DNA-binding one finger; eQTL, expression quantitative trait locus; FKF, flavin-binding, kelch repeat, F-box 1; *FLC*, flowering locus C; *FT*, flowering locus T; *GI*, gigantea; GO, gene ontology; HRM, high-resolution DNA melting; LOD, logarithm of odds; LS, least squares; MeV, multiexperiment viewer; PCR, polymerase chain reaction; QTL, quantitative trait locus; RNA, ribonucleic acid; SA, salicylic acid; SNP, single nucleotide polymorphism.

Plant Genome 11:170040
doi: 10.3835/plantgenome2017.05.0040

host range, including potato (Inderbitzin et al., 2011). Blockage of the xylem occurs with infection reducing the flow of water and nutrients, which is associated with wilting and chlorosis (Fradin and Thomma, 2006). Defense responses in the plant include production of tyloses in the xylem to block the flow of conidia and production of antifungal defense compounds and enzymes (Beckman, 1964; Daayf, 2015; Talboys, 1972; Yadeta and Thomma, 2013). In potato, *Verticillium* infection also induces early vine maturity (Rowe and Powelson, 2002). Potato vine maturity is a form of whole plant senescence, which is coordinated with production of tubers (Davies and Gan, 2012; Ewing and Struik, 1992; Wohleb et al., 2014). *Verticillium*-induced early vine maturity results in smaller vines with reduced resources available for transfer to tubers leading to significantly decreased yields (Rowe and Powelson, 2002).

Tubers develop from modified underground stems called stolons. Under inductive conditions, stolon tips will undergo swelling to form tubers (Ewing and Struik, 1992). Andean varieties, such as *S. tuberosum* spp. *andigena*, and wild potato species are strictly dependent on short days for tuberization; however, *S. tuberosum* spp. *tuberosum*, derived from Chilean landraces, has the capacity to tuberize under long days (Rodriguez-Falcon et al., 2006). Grafting studies showed that short-day (long-night) length is sensed in the leaves followed by transport of mobile signals to the stolons (Chapman, 1958; Gregory, 1956). Recent studies show photoperiod control of the timing of tuberization by potato orthologs of flowering time regulators (Hannapel et al., 2017; Rodriguez-Falcon et al., 2006). *CONSTANS* (*CO*) in *Arabidopsis thaliana* is involved in promoting flowering under long days through regulation of expression of *flowering locus T* (*FT*) (Shim et al., 2017; Turck et al., 2008). The FT protein is a mobile florigen produced in leaves in response to long days and mobilized to floral meristems. In potato, conversely, *CO* suppresses tuberization under long days in *S. tuberosum* spp. *andigena* (González-Schain et al., 2012; Martínez-García et al., 2002). The potato *FT* ortholog, *StSP6A*, was found to be a mobile tuberigen in response to short daylengths (Navarro et al., 2011). In the regulatory pathway upstream, another *FT*-like gene, *StSP5G*, is a negative regulator of *StSP6A* gene expression, but the mechanism of repression is not known (Abelenda et al., 2016). The potato *CO* orthologs, *StCOL1* and *2*, activate transcription of *StSP5G* in response to short days (Abelenda et al., 2016).

The *CDF1* transcriptional repressor downregulates expression of *CO* in *A. thaliana*, which results in a delay of flowering (Fornara et al., 2009). *CDF1* is targeted for degradation by the light-dependent interaction of *GIGANTEA* (*GI*) and *FLAVIN-BINDING, KELCH REPEAT, F-BOX1* (*FKF1*) to promote flowering (Imaizumi et al., 2005; Sawa et al., 2007). The potato ortholog, *StCDF1*, is similarly targeted for protein degradation under noninductive long days by the light-dependent interaction of potato orthologs of *GI* and *FKF1*; however, the result is to delay tuberization (Kloosterman et al., 2013). This interaction is lost under tuber-inducing short-day conditions resulting in increased StCDF1 protein levels and downstream signaling of increased StSP6A in stolons leading to tuberization. Potato clones demonstrating early maturity and tuberization under long days were found to carry variants of the *StCDF1*, *StCDF1.2*, and *StCDF1.3*, encoding truncated proteins missing domains for interaction of FKF1 (Kloosterman et al., 2013; Morris et al., 2014). These studies show the importance of StCDF1 in determining maturity and tuberization timing.

Tuberization is also regulated by BEL1-like transcription factors, which function together with KNOX-type transcription factors to regulate growth and development in plants (Hannapel et al., 2017). The potato *BEL-1* gene, *StBEL5*, was also found to function as a mobile signal for tuberization, where the transcript was mobilized from the leaves to the stolons under short-day conditions (Banerjee et al., 2006; Chen et al., 2003). Studies have also shown that StBEL5 upregulates *StCDF1* and *StSP6A* gene expression (Sharma et al., 2016). In addition, *CO* in potato was found to be a repressor of *StBEL5* expression (González-Schain et al., 2012). Other members of the BEL family, *StBEL11*, and *StBEL29*, were also found to express transcripts that mobilized from leaves to stolons under short days. These genes were antagonistic to *StBEL5* (Ghate et al., 2017) and were postulated to function in an activator/inhibitor module that fine-tunes tuber growth.

Flowering locus T has also emerged as an integrator of multiple signals for flowering (Pin and Nilsson, 2012). In *A. thaliana*, *Fusarium oxysporum* colonization of the xylem induces vascular wilt similar to *Verticillium*. Infection was also found to accelerate flowering time through regulating transcription of flowering time genes, *flowering locus C* (*FLC*), *FT*, and *GI* (Lyons et al., 2015). Accelerated flowering was observed with infection of *A. thaliana* with leaf colonizing pathogens *Pseudomonas syringae*, *Xanthomonas campestris*, and *Peronospora parasitica* (Korves and Bergelson, 2003). Furthermore, the salicylic acid (SA) regulator gene, *WIN3*, was found to confer resistance to *P. syringae* and *Botrytis cinerea* in concert with other SA regulators, in addition to affecting flowering regulators *FLC* and *FT* (Wang et al., 2011). Induction of early flowering or tuberization in the infected plant allows for reproduction before the pathogen kills the plant entirely. The trade-off for accelerated development is decreased production of fruits, seeds, and tubers (Rowe and Powelson, 2002; Su et al., 2013).

In tomato (*Solanum lycopersiucum* L.), QTL mapping of *Verticillium* wilt disease resistance led to identification of a single dominant locus, *Ve*, on chromosome 9 (Diwan et al., 1999). Race 1 of *V. dahliae* and *V. albo-atrum* pathogens are effectively mitigated by the *Ve* locus, but not race 2. Positional cloning of the tomato *Ve* locus identified two tandemly located, closely related genes encoding leucine-rich repeat cell surface receptors, *Ve1* and *Ve2* (Kawchuk et al., 2001). Potato orthologs of *Ve1* and *Ve2*

were cloned using polymerase chain reaction (PCR) and were demonstrated in diploid potato clones to map to chromosome 9 in a region corresponding to the location of *Ve* in tomato (Simko et al., 2003). Additionally, linkage disequilibrium mapping of tetraploid potato clones demonstrated that *V. dahliae* and *V. albo-atrum* resistance was associated with a marker that was closely linked to the ortholog of *Ve1* (Simko et al., 2004a, 2004b).

Wild *Solanum* species were found to be sources of *Verticillium* resistance and have been introgressed to *S. tuberosum* in potato breeding programs (Concibido et al., 1994; Corsini and Pavek, 1996; Corsini et al., 1988; Jansky and Rouse, 2000; Jansky et al., 2004; Lynch et al., 1997; Simko et al., 2004c). Development of markers to predict resistance to *Verticillium* wilt has involved PCR of the region conserved between *Ve1* and *Ve2* to clone orthologous *Ve* genes from several resistant wild *Solanum* species (Bae et al., 2008; Uribe et al., 2014). The cloned genes from the wild species were found to have high sequence identity with *Ve2*. The diploid potato clone 12120-03 was found to be heterozygous for a *Ve2* resistance allele and had low levels of *V. dahliae* pathogen and mild symptoms after infection (Tai et al., 2013). Another diploid potato clone, 07506-01, was homozygous null for *Ve2* resistance alleles; however, this clone did not develop symptoms even after high levels of *V. dahliae* were found after infection (Tai et al., 2013). These results suggested that 07506–01 had tolerance to *V. dahliae*.

The expression of genes can also be genetically mapped as eQTL (Druka et al., 2010; Holloway and Li, 2010). The eQTL are loci that control the expression of the genes either in *cis* (local regulation) or in *trans* (located at distant locations). The eQTL analysis was used to understand the genetic architecture underlying partial resistance to *Puccinia hordei* in barley (Chen et al., 2010) and diverse biological processes in tomato (Ranjan et al., 2016). To better understand the genetics underlying *V. dahliae* disease resistance, genetic mapping of the trait and eQTL was done using a biparental cross population derived from 12120-03 and 07506-01. The objective of the study was to identify gene networks involved in *V. dahliae* disease resistance in potato.

Materials and Methods

Plant Materials

Diploid potato clone 12120-03 was used as a female parent in a cross with male diploid parent 07506-01 to generate a F_1 mapping population (15143) consisting of 91 clones. The male parent, 07506-01, was derived from pollination of W9306.2, with bulked pollen from 2 × hybrids. The female parental clone, 12120-03 was derived from a cross between 09113 and 11 × 09753-01. The pedigree of both parental clones contains *S. phureja* and *S. stenotomum*. Disease-free seed tuber stocks of the potato clones were propagated in the field and maintained at the Benton-Ridge Substation of Agriculture and Agri-Food Canada in Benton, New Brunswick, Canada. The seed tubers from the clones were planted in an experimental field (45°52′ N, 66°31′ W) containing *V. dahliae* at the Fredericton Research and Development Centre of Agriculture and Agri-Food Canada in Fredericton, New Brunswick, Canada, on 22 May 2009. Planting in Fredericton was done in a randomized complete block design with three replicate plots of five hills (i.e., plants). Fertilizer was banded about 7.5 cm to each side and 5 cm below the potato seed pieces at planting according to normal production practices at 200 kg N ha^{-1} as ammonium nitrate, 150 kg P_2O_5 ha^{-1}, and 150 kg K_2O ha^{-1}. The plants were hilled in mid-July. Standard commercial practices were used for control of diseases, insects, and weeds. No irrigation was applied. The variety Green Mountain was planted in guard rows flanking the plot, every third row, and at the ends of each row. Green Mountain was tested for presence of *V. dahliae* at locations throughout the plot to confirm presence of the pathogen. Stem cuttings of Green Mountain plants were taken at the base of the stem and surfaced sterilized in 10% bleach, 70% ethanol, and 0.05% Tween 20 (Sigma-Aldrich, Oakville, Canada). Slices of sterilized stems (0.5 cm wide) were cut and placed on a sterile potato dextrose agar (Sigma-Aldrich, Oakville, Canada) in 10 cm Petri dishes for 1 to 2 wk at 20°C. Identification of *V. dahliae* cultures was based on visual characteristics.

The smallest leaflet of the fourth leaf from the top of the plant was sampled for ribonucleic acid (RNA) extraction from each of the five plants in each replicate plot 52 d after planting (DAP) for RNA extraction. The leaflets for each replicate were combined in a single 2 mL tube containing lysing matrix D (MP Biomedicals, Solon, OH) and immediately flash frozen in liquid nitrogen in the field. Frozen leaf material was stored at –80°C until processed.

Disease Resistance Scoring

Disease resistance was scored at 100 DAP. Visual scoring of disease resistance was done using an index from 1 to 9, where 1 was a dead plant and 9 was a fully upright healthy plant. Leaf yellowing, leaf loss, and wilting would result in lowered scores. The least squares (LS) mean of the disease resistance score was used for MapQTL analysis.

RNA Extraction

Leaf tissue was ground in the Lysing Matrix D tubes using a Geno Grinder 2000 (SPEX CertiPrep) machine for 2 min at speed 5. Samples were kept frozen. One mL RNA lysis buffer [200 mM sodium borate decahydrate (Borax), pH 9.0, 30 mM ethylene glygol bis(β-aminoethyl ether)-N-N′-tetraacetic acid, 1% (w/v) sodium dodecyl sulfate, and 10 mM dithiothreitol] plus 1% (w/v) sodium deoxycholate and 2% (w/v) polyvinylpyrrolidone (avg. molecular weight of 40,000; Luo et al., 2011; Wan and Wilkins, 1994) was added to ground leaf tissue in each tube. The lysate was mixed using a vortexer and centrifuged briefly at 10,000 × *g* for 5 min to pellet debris. Lysate supernatant (200 µL) was used for RNA extraction using the Agencourt RNAdvance Tissue Kit (Beckman

Coulter, Mississauga, Canada) according to manufacturer's instructions for liquid samples.

Deep Serial Analysis of Gene Expression

Two micrograms of total RNA per sample was used to construct deep serial analysis of gene expression (DeepSAGE) tag libraries (Nielsen et al., 2006) using a modification to facilitate direct sequencing of the amplicons by Illumina sequencing. The samples from 91 clones were bar-coded with a different identification key. Samples were diluted to a final concentration of 10 nM and were pooled. Each of the three biological replicates was done in a separate pool. Final pool concentrations were estimated using Quant-iT-PicoGreen prior to template DNA hybridization and sequencing on an Illumina Genome Analyzer II (Illumina, San Diego, CA) according to the manufacturer's instructions. Due to the restriction enzyme *Nla*III used for library construction, each tag carries the nucleotides CATG at the 5′ end.

Tag count data were transformed into a data matrix using in-house Perl scripts and transformed to the relative unit of counts per million. Tags included in the analysis had to be present in at least one biological replicate and had to have a count of at least three. Clonal variation between samples was detected (p-value ≤ 0.05) using the exact test for a negative binomial distribution from the Bioconductor (release 3.5) package EdgeR (Robinson et al., 2010) implemented in the R (v.3.2.5; R Core Team, 2016). Tags that did not have significant clonal variation were removed, leaving 6248 tags. The LS mean was calculated for each tag for each clone. The 21-nt tag sequences were aligned against PGSC *S. tuberosum* group Phureja DM1-3 transcripts (v.3.4) at Spud DB (Hirsch et al., 2014) using blastn. Hits with E-value ≤ 0.5 were filtered in. Where there were multiple blast hits meeting E-value criteria, only the one with the longest alignment was included. 4198 tags were assigned single-hit annotations in this manner and were used for eQTL analysis (Supplementary Table S1). The remaining 2050 tags without hits meeting the criteria or with multiple hits with the same E-value and length of alignment were not included in the eQTL analysis. The tag count data was deposited at the NCBI GEO database accession number GSE107936.

Nanostring nCounter Analysis of Gene Expression

Multiplex analysis of the expression of *StSP5G* and *StCOL1/2* were examined using a nCounter Digital Analyzer (Nanostring Technologies, Seattle, WA). Details of nCounter multiplex gene expression analysis are described elsewhere (Geiss et al., 2008). The same RNA samples used for DeepSAGE were also used for nCounter analysis. Gene expression of six housekeeping genes 18S rRNA, aprt, cyclophilin (Nicot et al., 2005; Tai et al., 2009), elongation factor 1-α (EF-1-α; Nakane et al., 2003) and cox1-B (Li et al., 2010; Quinones et al., 1995) was also measured and the geometric mean of their expression was used to normalize gene expression values (de Almeida et al., 2015; Luo et al., 2011). The probes used for the nCounter analysis are provided in Supplementary Table S2.

DNA Extraction and Genotyping

Fresh leaf material (100 mg) from plants grown in the greenhouse for one month was pulverized in 2 mL lysing matrix "A" tubes (MP Biomedicals), using a FastPrep FP 120 for 40 s in 750 µL of the following extraction buffer: 1.4 M NaCl, 20 mM EDTA, 2% CTAB (w/v), 0.1 M Tris pH 8.4, and 1% 2-mercaptoethanol (v/v). The DNA suspension was incubated 60 min at 60°C after which it was mixed 1:1 with chloroform/isoamyl alcohol (24:1 v/v), and then centrifuged at 13,148g for 5 min. The supernatant was collected and 5 M NaCl added in a 1:40 v/v ratio before precipitation in 95% ethanol for 30 min at –20°C. The DNA was centrifuged at 13,148g for 10 min and the pellet washed in 70% ethanol followed by centrifugation for 5 min. The DNA was suspended in 150 µL sterile distilled water and treated with 1.5 µL of 10 mg/ml DNase-free RNase.

Polymerase chain reaction and high-resolution DNA melting (HRM) analysis of genetic mapping anchor markers was done according to De Koeyer et al. (2010). Primer sequences and locations of anchor markers are found in Supplementary Table S3. Diversity Arrays Technology P/L of Canberra, Australia, provided services for genotyping the 91 diploid potato progeny clones using methods described by Wenzl et al. (2004). Diversity array technology (DArT) markers were analyzed similarly to Sharma et al. (2013). Briefly, DNA from each clone was double digested with restriction enzyme *Pst*I and *Taq*I ligated to *Pst*I adaptors then amplified by PCR. The PCR products were Cy3 labeled and hybridized together with a Cy5-labeled reference to a high-resolution potato genotyping array containing 7680 DArT probes (Sliwka et al., 2012). Arrays were scanned to detect fluorescence intensity at each probe. The data from the scanned images were extracted and analyzed using the DArTsoft 7.4 software (Diversity Arrays Technology P/L, Canberra, Australia). The SolCap 8303 Infinium Chip was used for single nucleotide polymorphism (SNP) genotyping using a procedure described in Felcher et al. (2012). The probe sequences and SNP information are available at http://solcap.msu.edu/potato_infinium.shtml [verified 13 Nov. 2017]. Genotyping of the *Solanum tuberosum* CYCLING DOF FACTOR (CDF, with DOF meaning DNA-binding one finger) family member, *StCDF1*, was done using a HRM marker (Supplementary Table S3). Cleaved amplified polymorphic sequence (CAPS) genotyping for the *Ve2* gene was done using the *Ve2* marker according to Uribe et al. (2014).

Linkage Mapping, QTL, and eQTL Analysis

Low quality and noninformative SNPs were removed prior to mapping using JoinMap 4.1 for linkage mapping with population type CP (cross-pollination) with <hkxhk>, <lmxll>, and <nnxnp> segregation and markers were grouped by regression mapping using Haldane's function (Kyazma B.V., Wageningen, the Netherlands). Parents were phased and loci coded according to the type of segregation as per the requirement of JoinMap. The LS mean of the disease resistance score was used for QTL analysis using MapQTL 6 (Kyazma B.V., Wageningen, the Netherlands).

For analysis of DeepSAGE gene expression, the $\log_2$ ratio of the LS mean tag count over the LS mean tag count for clone 07506-01 was used for composite interval mapping with MapQTL6 (Kyazma B.V., Waganingen, the Netherlands). The LS mean of $\log_2$–transformed normalized nCounter gene expression values were used for analysis. The logarithm of odds (LOD) scores across linkage groups for all QTL and eQTL were averaged over 1-cM intervals for the all the tags and disease resistance and were placed in a single data matrix. Multiexperiment viewer (MeV) was used to analyze the pattern of eQTLs across the linkage groups. Hierarchical clustering of tags was done using the Pearson correlation matrix and average linkage clustering. Heat maps of LOD scores across linkage groups were also generated using MeV.

Tags with eQTL at *StCDF1* and *Ve2* loci were identified by averaging LOD scores for intervals that were within ±1 cM from the mapped location of the *StCDF1* and *Ve2*. Those tags with average LOD scores over the intervals greater than three were identified. Lists of tags with *StCDF1* and *Ve2* eQTL were compared using Genowiz 4.0 (Ocimum Biosolutions, Indianapolis, IN). Lists of tag with eQTL for *StCDF1* only, *Ve2* only, or *StCDF1* and *Ve2* were made. Enrichment analysis for associated GO terms was performed using the topGO (v.2.28.0; Alexa and Rahnenfuhrer, 2010) in R version 3.2.5 (2016). The Revigo webtool (http://revigo.irb.hr/, verified 15 Nov. 2017) was used to produce graph-based visualization of GO network (Supek et al., 2011)

Epistasis Analysis

Epistasis between the *StCDF1* and *Ve2* loci in the regulation of disease resistance and gene expression was tested using the FRGEpistasis package (https://www.bioconductor.org/packages/release/bioc/html/FRGEpistasis.html, verified 17 Nov. 2017; Zhang et al., 2014) in R v.3.2.5 (2016). FRGEpistasis uses the physical map locations of *StCDF1* and *Ve2* for analysis of epistasis. ANOVA with general linear model was used to analyze differences in disease resistance and gene expression for *StCDF1*, *StSP5G*, and *StSP6A* between genotypic combinations of *StCDF1* and *Ve2* and Duncan's test was used for pairwise comparisons between genotypes using SYSTAT 13 (Systat Software, Inc., San Jose, CA).

Cloning of *StCDF1* Alleles

Rapid amplification of cDNA ends (RACE) was used to clone full-length cDNA for h and k alleles from hh and kk homozygous clones, respectively. The SMARTer RACE 5′/3′ kit (Clontech, Inc., Mountain View, CA) was used with total RNA from leaves according to manufacturer's instructions. A second round of PCR was done with nested primers. The gene specific primer for 5′ RACE was 5′GATTACGCCAAGCTTTCGGCGACCAGATCCCACAGGCACAT (5′GSP) and the nested gene specific primer for secondary PCR was 5′GATTACGC-CAAGCTT-TTCTCATTGTCC CTCCAGCAGTCC (5′ NGSP2). The gene specific primer for 3′ RACE was 5′GATTACGCCAAGCTT CCAGCCTC-GTTACTTCTGCAAGAACTGCCA (3′GSP1) and the nested primer was 5'GATTACGCCAAGCTTGCCAGAG ATATTGGACTGCTGGAGGGAC (3′ NGSP2).

5′ and 3′ RACE PCR products were ligated into the pCR4 TOPO TA cloning vector (Thermo Fisher, Waltham, MA) according to manufacturer's instructions. Plasmids were transformed into *Escherichia coli* using electroporation. Colonies were grown on kanamycin plates and 12 were picked for Sanger sequencing with M13 forward and M13 reverse primers on the Applied Biosystem's 3730xl DNA Analyzer at the McGill Genome Quebec Innovation Centre (Montreal, Canada). Assembly of sequences was done using Lasergene 12 Core Suite (DNASTAR, Madison, WI). Multiple sequence alignment with the StCDF1.1 and StCDF1.2 protein sequence (Kloosterman et al., 2013) was done using Clustal W.

Results

Disease Resistance QTL

A linkage map was constructed from 1602 markers, including 1023 SNP, 545 DArT, and 34 HRM loci (Supplementary Fig. S1). The distribution of the LS mean of the *Verticillium* disease resistance score for the 91 progeny at 100 DAP is shown in Fig. 1. QTL mapping of disease resistance was performed and LOD scores were averaged over 1 cM intervals and the distribution of QTL over all linkage groups was examined. Chromosomes 5 and 9 had QTL peaks with LOD scores over three (Fig. 2). The QTL with the highest LOD score was on chromosome 5 which accounted for 48.2% of the explained variance. The genetic location of markers near QTL for disease resistance was

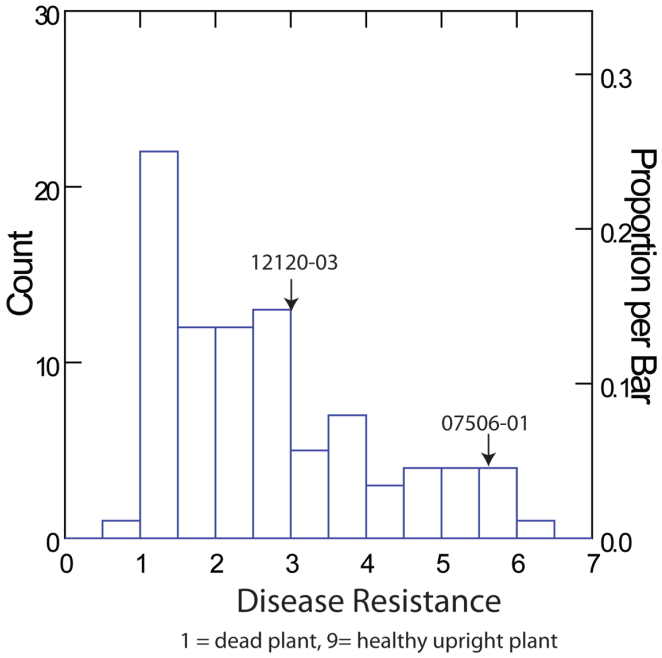

Fig. 1. Distribution of disease resistance. Least squares mean of disease resistance scored at 100 d after planting for Population 15143. Parental disease resistance scores are indicated by arrows.

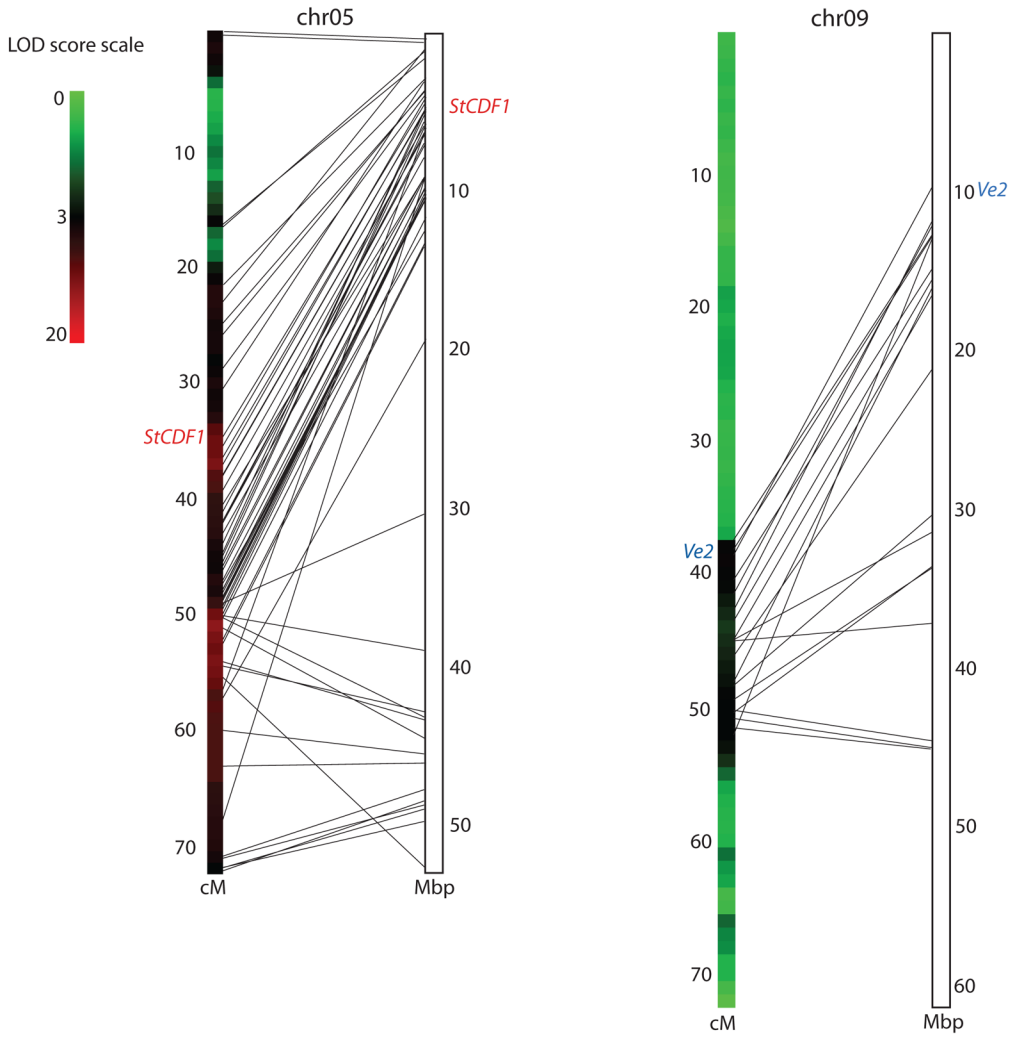

Fig. 2. Genetic and physical maps of quantitative trait loci (QTL) for disease resistance on chromosomes 5 and 9. Lines link location of markers within 1 cM of the disease resistance QTL on genetic and physical maps. The locations of *StCDF1* and *Ve2* genes are indicated. The logarithm of odds (LOD) scores across the genetic map are indicated by a color scale.

compared to the physical location. The order of the markers was highly similar to the physical map; however, the distance between markers on the end of chromosomes was higher in the genetic map. An explanation for this is the tendency in plant chromosomes for higher rates of recombination in subtelomeric regions and lower rates of recombination in centromeric regions (Mézard, 2006).

The QTL on chromosome 5 included one which covered the *StCDF1* gene (Fig. 2 and 6a) that encodes a cycling DOF transcriptional repressor which controls timing of maturity and tuberization in potato (Kloosterman et al., 2013). To verify location of the *StCDF1* gene in the QTL interval, a HRM genotyping assay was used (Supplementary Table S3). Genetic mapping using the *StCDF1* HRM marker confirmed the location of the gene (Fig. 2). The *StCDF1* HRM primer was located between the DNA binding and the GI binding domains. The two alleles of *StCDF1* in the 15143 population were named h and k.

The QTL on chromosome 9, which accounted for 17% of the explained variance, included the locus for the *Ve2*, *Verticillium* wilt resistance gene (Kawchuk et al., 2001). The genetic map location of the *Ve2* gene was confirmed using a CAPS marker (Uribe et al., 2014; Fig. 2). Clone 12120-03 was heterozygous for the *Ve2* resistance allele (uv) and 07506-01 did not carry resistance alleles (uu; Tai et al., 2013).

Sequencing of *StCDF1* h and k Alleles

RACE was used to clone the *StCDF1* full-length cDNA for the h and k alleles of population 15143. The cDNA sequence analysis indicates that the HRM marker detected a synonymous nucleotide variant (data not shown). Protein sequence alignment demonstrated that the k allele encoded StCDF1.1 (Fig. 3). The h allele encoded a protein with a modified C terminal end that was missing the *FKF1* binding domain and was identical to StCDF1.3 (Kloosterman et al., 2013). The HRM genotyping of *StCDF1* for the two diploid parents of the 15143 population, clones 12120-03 and 07506-01, showed that both were heterozygous for *StCDF1* alleles (data not shown).

Epistasis between *Ve2* and *StCDF1*

The cross of 12120-03 (hk × uv) and 07506-01 (hk × uu) resulted in progeny clones that carried all three genotypic combinations of h and k allele alleles of the *StCDF1* gene (hh, hk, and kk); however, there were only two possible *Ve2* genotypic combinations, uv and uu. This resulted in six genotypic combinations of *StCDF1* and *Ve2* alleles: hh*uu, hh*uv, hk*uu, hk*uv, kk*uu, and kk*uv. The average disease resistance score for *StCDF1* and *Ve2* genotypes is shown in Fig. 4. Presence of the k allele of *StCDF1* was associated with increased disease resistance compared with hh homozygotes (Fig. 4a).

Examination of the *Ve2* resistance allele showed that disease resistance was not significantly different between uu and uv clones in the ANOVA analysis (Fig. 4b). Disease resistance was reduced in hh × uv versus the hh × uu genotypes; however, the *Ve2* resistance allele did not have significant effects on clones carrying k allele (Fig. 4c). The difference in disease resistance in the hh × uv versus the hh × uu genotypes was also small in comparison with the differences between hh, hk, and kk genotypes. The effectiveness of the *Ve2* resistance allele in increasing disease resistance was dependent on the genotype of *StCDF1*, which indicated epistasis. The results also indicate that *StCDF1* functions downstream of *Ve2*. Epistatic interaction between the *StCDF1* and *Ve2* genes was tested using a functional regression model (Zhang et al., 2014). Highly significant interaction with a p value of 1.83×10^{-5} was found between the *StCDF1* and *Ve2* in the control of *V. dahliae* disease resistance.

eQTL Analysis

Biological functions affected by *StCDF1* and *Ve2* loci at the molecular and cellular levels can be explored using eQTL analysis. eQTL analysis involved quantification of gene expression across Population 15143 and genetic mapping of the QTL for expression each gene. DeepSAGE (Nielsen et al., 2006) was used for genome-wide gene expression analysis across the 91 progeny clones of Population 15143. The DeepSAGE analysis produced 4198 unique tags that were derived from 2210 genes (some tags were derived from different regions of the same gene). A heat map of LOD scores for the eQTL for each of the tags across linkage groups was generated. The genes and their LOD score heat maps were ordered based on their physical location in the genome (Fig. 5). The majority of the high LOD scores were found along the diagonal of the heat map matrix. These results indicated that for most genes the eQTL controlling expression was mapped near the gene (*cis*-eQTL). This is characteristic of eQTL analyses (Druka et al., 2010; Holloway and Li, 2010) and indicated compatibility of tag count gene expression data for eQTL mapping. There were also many *trans*-eQTLs, where eQTLs for a gene were found on another chromosome. There were a high number of *trans*-eQTLs found on chromosome 5 indicating the presence of a master regulator of gene expression. The genome-wide pattern of eQTL was similar to results published by others using microarray data (Kloosterman et al., 2012) indicating that tag count gene expression data could produce similar results as microarrays. Inclusion of tags that were not unique to a single gene resulted in reduced *cis*-eQTLs (data not shown). Therefore, only unique tags were used.

```
StCDF1.1  MSEVRDPAI KLFGKTI GMTQQETNCVYLHDDHTTSSPLSI DDDKI TLEGE  50
StCDF1.2  MSEVRDPAI KLFGKTI GMTQQETNCVYLHDDHTTSSPLSI DDDKI TLEGE  50
 h allele MSEVRDPAI KLFGKTI GMTQQETNCVYLHDDHTTSSPLSI DDDKI TLEGE  50
 k allele MSEVRDPAI KLFGKTI GMTQQETNCVYLHDDHTTSSPLSI DDDKI TLEGE  50

StCDF1.1  FTQSKQDDELVDPTADSSI EPETSSGI SDDI KMQDADKETLSSKSI EEED 100
StCDF1.2  FTQSKQDDELVDPTADSSI EPETSSGI SDDI KMQDADKETLSSKSI EEED 100
 h allele FTQSKQDDELVDPTADSSI EPETSSGI SDDI KMQDADKETLSSKSI EEED 100
 k allele FTQSKQDDELVDPTADSSI EPETSSGI SDDI KMQDADKETLSSKSI EEED 100

StCDF1.1  SSEEKALKKPDKLI PCPRCNSMETKFCYYNNYNVNQPRYFCKNCQRYWTA 150
StCDF1.2  SSEEKALKKPDKLI PCPRCNSMETKFCYYNNYNVNQPRYFCKNCQRYWTA 150
 h allele SSEEKALKKPDKLI PCPRCNSMETKFCYYNNYNVNQPRYFCKNCQRYWTA 150
 k allele SSEEKALKKPDKLI PCPRCNSMETKFCYYNNYNVNQPRYFCKNCQRYWTA 150

StCDF1.1  GGTMRNVPVGSGRRKNKSSSI SNYPLQAGRVEAAAHGMHLPALRTNGTVL 200
StCDF1.2  GGTMRNVPVGSGRRKNKSSSI SNYPLQAGRVEAAAHGMHLPALRTNGTVL 200
 h allele GGTMRNVPVGSGRRKNKSSSI SNYPLQAGRVEAAAHGMHLPALRTNGTVL 200
 k allele GGTMRNVPVGSGRRKNKSSSI SNYPLQAGRVEAAAHGMHLPALRTNGTVL 200

StCDF1.1  TFGSDKPLCDSMVSALNLAENSHNMNRNEFHGSERRMPAI GNDQSNGTCS 250
StCDF1.2  TFGSDKPLCDSMVSALNLAENSHNMNRNEFHGSERRMPAI GNDQSNGTCS 250
 h allele TFGSDKPLCDSMVSALNLAENSHNMNRNEFHGSERRMPAI GNDQSNGTCS 250
 k allele TFGSDKPLCDSMVSALNLAENSHNMNRNEFHGSERRMPAI GNDQSNGTCS 250

StCDF1.1  TASSVTDKESSAGTHDLANWNNFQPFPPQVPYFQGAPWPYSGFPVSFYPA 300
StCDF1.2  TASSVTDKESSAGTHDLANWNNFQPFPPQVPYFQGAPWPYSGFPVSFYPA 300
 h allele TASSVTDKESSAGTHDLANWNNFQPFPPQVPYFQGAPWPYSGFPVSFYPA 300
 k allele TASSVTDKESSAGTHDLANWNNFQPFPPQVPYFQGAPWPYSGFPVSFYPA 300

StCDF1.1  TPYWGCTVANPWNVPWLSSDQSSVQNNSPTSPTLGKHSRDESKI DPSQSR 350
StCDF1.2  TPYWGCTVANPWNVPWLSSDQSSVQNNSPTSPTLGKHSRDESKI DPSQSR 350
 h allele TPYWGCTVANPWNVPWLSSDQSSVQNNSPTSPTLGKHSRDESKI DPSQSR 350
 k allele TPYWGCTVANPWNVPWLSSDQSSVQNNSPTSPTLGKHSRDESKI DPSQSR 350

StCDF1.1  RRDANLQNREGERCVLI PKTLRI HDPNEAAKSSI WSTLGI RNEKI DSARG 400
StCDF1.2  RRDANLQNREGERCVLI PKTLRI HDPNEAAKSSI WSTLVTRYQE.      395
 h allele RRDANLQNREGERCVLI PKTLRI HDPNEAAKSSI WSTLG----------  389
 k allele RRDANLQNREGERCVLI PKTLRI HDPNEAAKSSI WSTLGI RNEKI DSARG 400

StCDF1.1  TMLFSAFNPKADHRNREHDTSFALQANPAALSRSLHFRESTQ.          443
StCDF1.2                                                      395
 h allele ---------KAGHRTG---------MGPPDRNEPEPDRNGTV.        414
 k allele TMLFSAFNPKADHRNREHDTSFALQANPAALSRSLHFRESTQ.          443
```

Fig. 3. Protein sequences of h and k alleles of *StCDF1*. The sequences were aligned with *StCDF1.1* and *StCDF1.2* sequences.

Gene Ontology Analysis of Genes with eQTL at *Ve2* and *StCDF1*

Genes involved in functions connected to *Ve2* or *StCDF1* would have eQTL at these loci. Tags with eQTL LOD scores over three at the *Ve2* and *StCDF1* loci were identified. eQTL LOD scores over three at the *Ve2* locus were observed for 103 tags (Fig. 6b, Supplementary Table S4). Among the 103 tags, 41 of the tags were aligned with the same gene, so that there were a total of 59 unique genes in the analysis. There were 505 tags representing 278 unique genes that had eQTL LOD scores over three at the *StCDF1* locus (Fig. 6c, Supplementary Table S5). There were nine genes that had eQTL at both the *StCDF1* and *Ve2*: TAG3032 (peptidase, trypsin-like serine and cysteine proteases), TAG1880 (sulfate adenylyltransferase), TAG5170 (Photosystem I reaction center subunit IV B Isoform 2), TAG296 (alcohol dehydrogenase), TAG1634 (S-adenosylmethionine synthase 2), TAG2483 (carbonic anhydrase), TAG2984 (gene of unknown function), and TAG5908 (Photosystem II 5 kDa protein, chloroplastic). The GO annotations of genes with eQTL at the *Ve2* or *StCDF1* loci were examined. The GO annotations with p-values ≤ 0.01 are listed in Supplementary Table S6. The

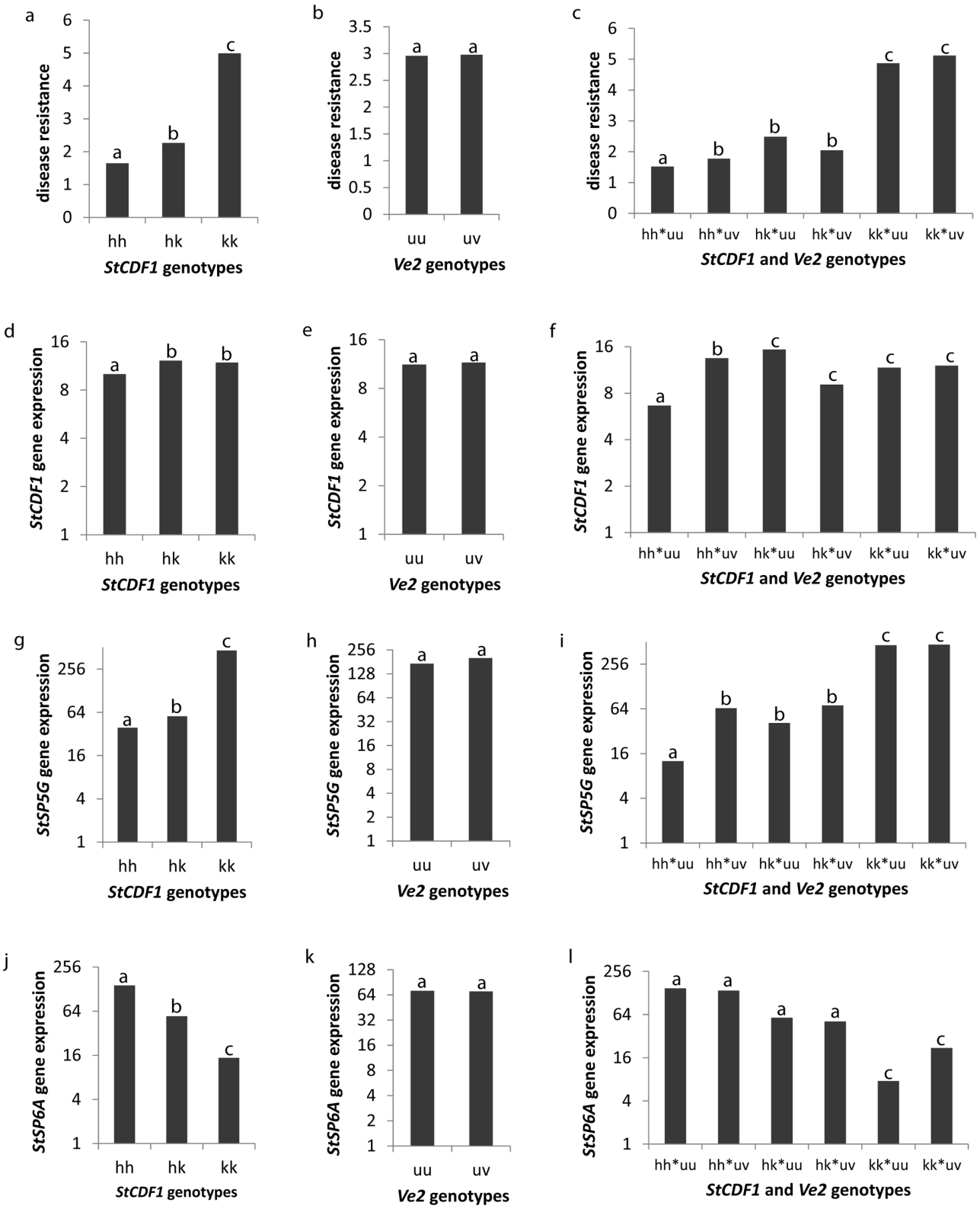

Fig. 4. Comparisons of disease resistance and gene expression between *StCDF1* and *Ve2* genotypes. The *StCDF1.1h* allele was labeled "h" and the *StCDF1.1k* allele was labeled "k." The resistance allele for *Ve2* was labeled "v" and the susceptible allele was "u". Disease resistance scores averaged for genotypes of (a) *StCDF1*, (b) *Ve2* and (c) genotype combination of *StCDF1* and *Ve2*. *StCDF1* (TAG2322) gene expression averaged for genotypes of (d) *StCDF1*, (e) *Ve2* and (f) genotype combination of *StCDF1* and *Ve2*. *Flowering locus T StSP5G* gene expression averaged for genotypes of (g) *StCDF1*, (h) *Ve2* and (i) genotype combination of *StCDF1* and *Ve2*. *Flowering locus T StSP6A* (TAG4626) gene expression averaged for genotypes of (j) *StCDF1*, (k) *Ve2* and (l) genotype combination of *StCDF1* and *Ve2*. ANOVA was done to find significant genotypic variation and pairwise comparisons were done using Duncan's test. Genotypes with significant differences in disease resistance scores are indicated by different letters above the bars.

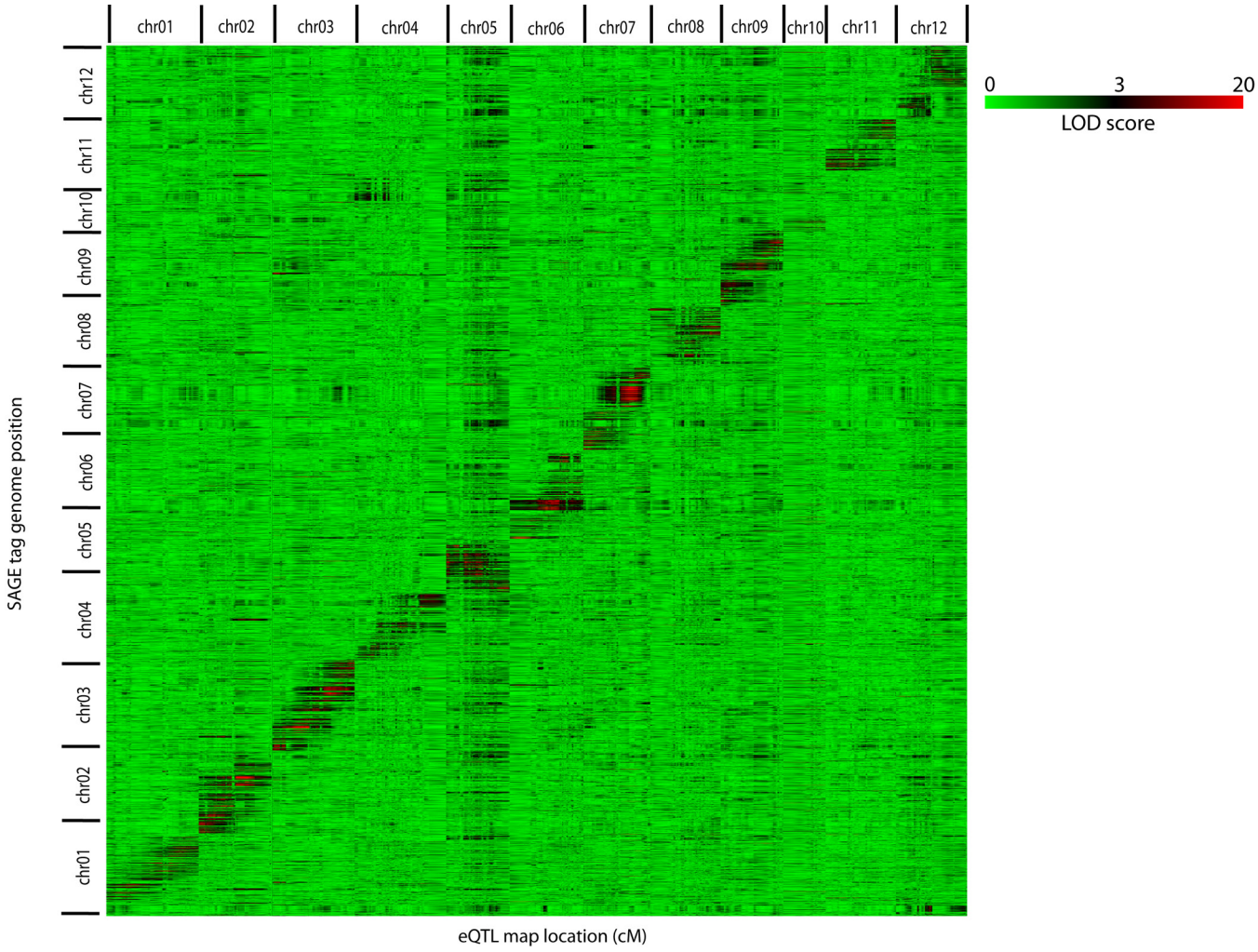

Fig. 5. Heat map of logarithm of odds (LOD) scores for expression quantitative trait loci (eQTL) across linkage groups. The physical locations of the genes are indicated on the left and the genetic locations of eQTL controlling expression of the genes are indicated across the top. The LOD scores are indicated by a color scale.

largest number of significant GO annotations was for biological process. Figure 7 shows the interactive graphs from the Revigo analysis. *Photosynthesis* was the GO term with the lowest *p*-value for both groups of genes. These results indicate that both *StCDF1* and *Ve2* loci affect photosynthesis. *Carotenoid biosynthesis*, *response to inorganic substance*, and *glyceraldehyde-3-phosphate metabolism* were other GO terms present in both groups. There were many GO terms unique to genes with eQTL at *StCDF1* or *Ve2*. Of interest were the GO terms *defense response to fungus*, *incompatible interaction*, *plant-type primary cell wall biogenesis*, and mitochondrial electron transport GO terms for genes with eQTL at the *Ve2* but not the *StCDF1* locus. Also of interest was the GO term, *response to oxidative stress*, that was present for genes with eQTL at *StCDF1* but not *Ve2*. In general, there were more genes with eQTL at the *StCDF1* locus producing more GO terms, but the terms associated with photosynthesis were highly significant.

eQTL of Genes in Tuberization Pathway

TAG4626 corresponded to the flowering time ortholog of *FT*, *StSP6A*. eQTL for TAG4626 were found on chromosome 5 and included the *StCDF1* locus, which correlates with the regulation of *StSP6A* by *StCDF1* (Fig. 6a). The eQTL on chromosome 5 accounted for 58.1% of the explained variance. Tags for *StSP5G* and *StCOL1* and *StCOL2* were not found among the 4198 tags; therefore, the nCounter analysis was used to quantify expression of these genes. *StCOL1* and *StCOL2* sequences were highly similar and the nCounter probe for *StCOL1/2* could hybridize to both genes. The nCounter data indicates that *StCOL1/2* gene expression was not detectable and eQTL were not found (data not shown). The reason may be that *StCOL1* and *StCOL2* gene expression peaks at the beginning of the day, and the samples were taken in the afternoon when expression was low. Expression of *StSP5G* was detected and eQTL analysis was done. The eQTL for *StSP5G* found on chromosome 5 (44.4% explained variance) overlapped with the eQTL for *StSP6A* including the *StCDF1* locus (Fig. 6a), which concurs with regulation of *StSP5G* by the *StCDF1* regulatory pathway.

The StCDF1 protein is regulated by protein degradation by *GI* and *FKF1* (Kloosterman et al., 2013).

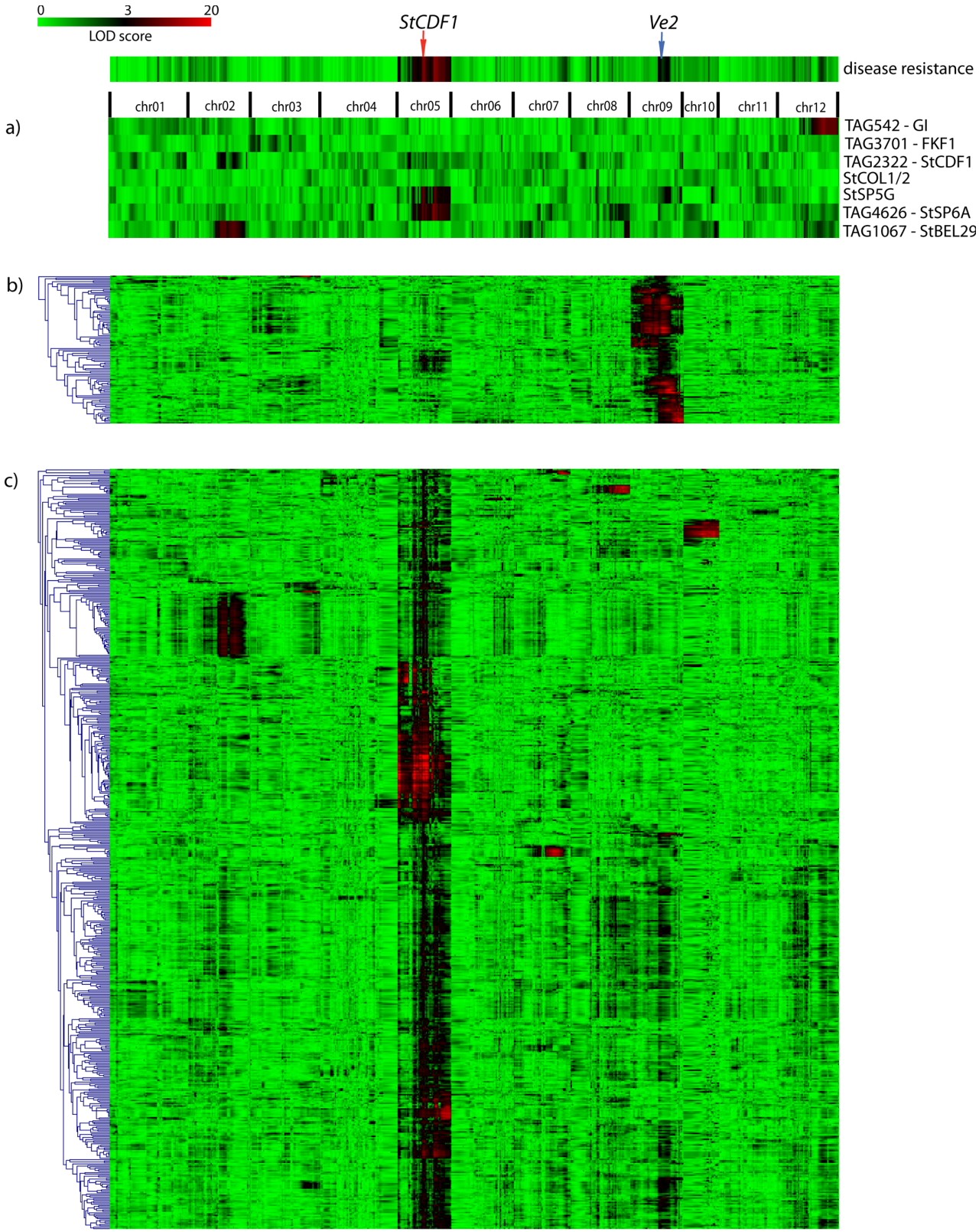

Fig. 6. Heat maps of logarithm of odds (LOD) scores for expression quantitative trait loci (eQTL) at *Ve2* and *StCDF1* loci. The heat map for LOD scores for disease resistance QTL across linkage groups are shown at the top of the figure. The arrows indicate locations of the *StCDF1* and *Ve2* genes. (a) eQTL for genes in the *StCDF1* pathway TAG542 (*Gigantea*, PGSC0003DMT400048370), TAG3701 (*FKF1*, PGSC0003DMT400051416), TAG2322 (*StCDF1*, PGSC0003DMT400047370), *StCOL1/2* (PGSC0003DMT400026068), *StSP5G* (PGSC0003DMT400041726), TAG4626 (*StSP6A*, PGSC0003DMT400060057), and TAG1067 (*StBEL29*, PGSC0003DMT400063762). (b) eQTL at the *Ve2* locus, and (c) eQTL at the *StCDF1* locus. The genes were clustered using hierarchical clustering for (b) and (c). The dendrogram from hierarchical clustering of eQTL LOD scores is shown on the left for (b) and (c). The LOD scores are indicated by a color scale in the top left.

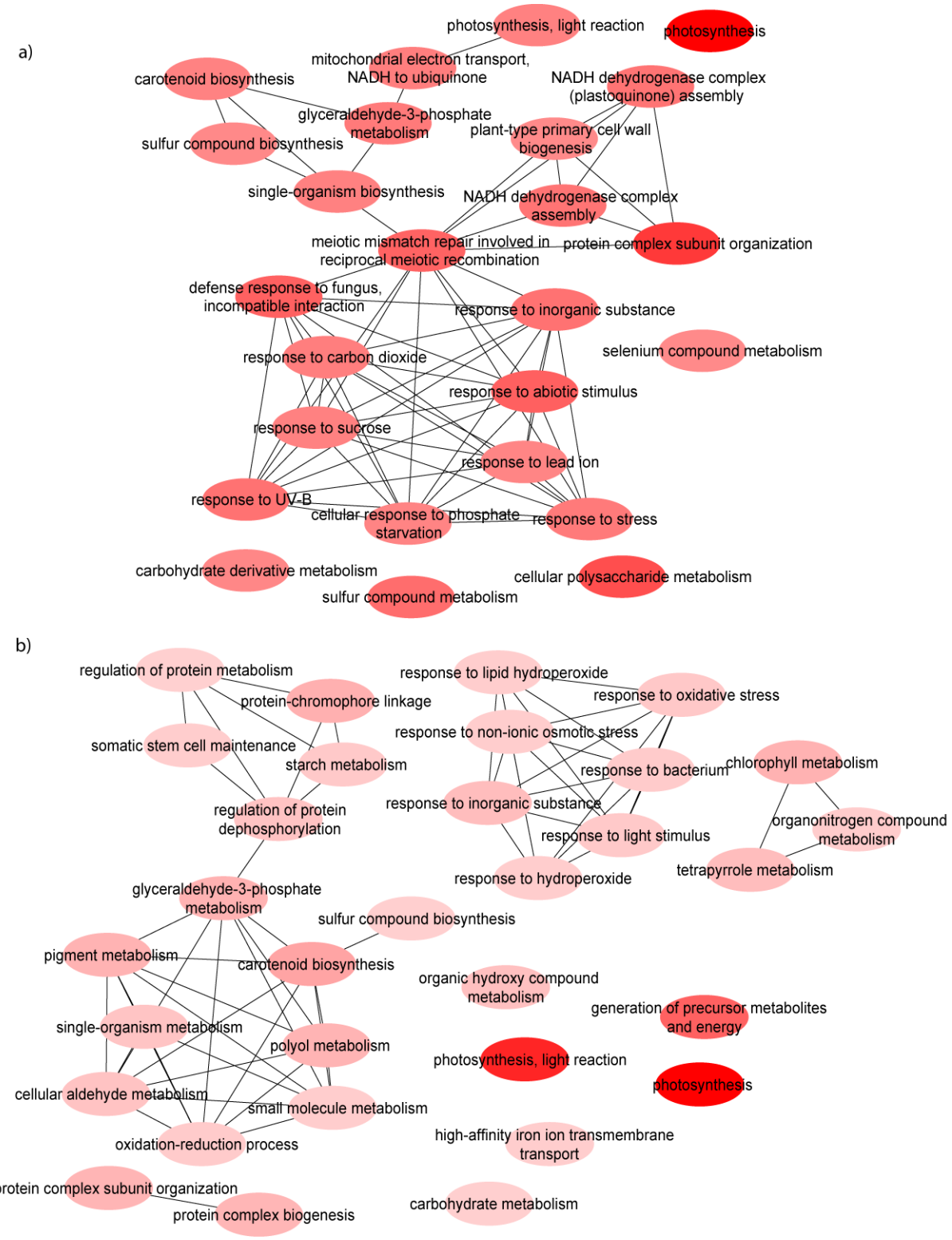

Fig. 7. Gene ontology (GO) annotations for genes with expression quantitative trait loci (eQTL) at (a) *Ve2* and (b) *StCDF1* loci. The intensity of the red color of the bubble for each GO term is negatively correlated with the *p*-value of the term. GO terms that are derived from the same genes are linked by lines.

TAG542 corresponded to *GI* and TAG3701 to *FKF1*. TAG542 had a major eQTL on chromosome 12 and TAG3701 on chromosome 3. The eQTL for *StCDF1* was also examined. There were *StCDF1* eQTL on chromosomes 1 and 2, with 19.2 and 21.8% explained variances, respectively (Fig. 6a) The *StBEL* genes are also involved in regulation of tuberization. *StBEL29* was found among the 4198 unique tags. The major eQTL for *StBEL29* was mapped to chromosome 2 in a similar region to the eQTL for *StCDF1* (Fig. 6a).

The differences between *StCDF1* and *Ve2* genotypes in gene expression of *StCDF1* and downstream genes *StSP6A* and *StSP5G* were compared to better understand the interaction between *StCDF1* and *Ve2* genes (Fig. 4d–l). There were significant effects of the *StCDF1* genotype on the expression of the three genes (Fig. 4d, g, i, j, and l), but the *Ve2* genotypes did not have significant differences (4e, h, k). When interactions between *StCDF1* and *Ve1* were examined, *StCDF1* and *StSP5G* expression in hh backgrounds were affected by the presence of the *Ve2* resistance allele (Fig. 4f, i). However, expression of *StSP6A* was not affected by *Ve2* genotype, even in the hh background (Fig. 4k, l). Expression levels of the *StCDF1* k allele were found to be higher than the h allele (Fig. 4 g, i). However, posttranslational regulation by protein degradation is a significant, so transcript levels do not reflect levels of protein and transcription repressor activity (Kloosterman et al., 2013). The expression of *StSP5G* and *StSP6A* were increased and decreased, respectively, in the presence of the k allele (Fig. 4i, l), which were consistent with the repressive action of *StSP5G* on *StSP6A* expression.

Discussion

Quantitative trait locus mapping of *Verticillium* wilt resistance identified a region of chromosome 9 that included the *Ve2* resistance gene. This result concurs with QTL previously reported in genetic mapping of *Verticillium* disease resistance in tomato (Diwan et al., 1999; Kawchuk et al., 2001) and potato (Simko et al., 2003; Simko et al., 2004a, 2004b). In addition, the results show that the major QTL for disease resistance identified in this study was not on chromosome 9, but on a region of chromosome 5 that included the *StCDF1* gene, which was shown to control tuberization in potato (Kloosterman et al., 2013). eQTL for tuberization regulators *StSP6A* and *StSP5G*, which are transcriptionally regulated by *StCDF1*, overlap with disease resistance QTL on chromosome 5. These results provide evidence for a role for the tuberization pathway in *V. dahliae* disease resistance in potato. Development of tubers is tightly coordinated with vine maturity (Davies and Gan, 2012; Ewing and Struik, 1992; Kloosterman et al., 2013; Thomas, 2013; Wohleb et al., 2014) and studies done by others have also found that a portion of *V. dahliae* resistance could be attributed to variation in vine maturity (Jansky and Miller, 2010; Simko and Haynes, 2016; Simko et al., 2004c). However, linkage of disease resistance to chromosome 5 described here is novel. QTL chromosome 5 may have been missed in previous studies that used candidate gene approaches focused on association of the *Ve* locus to *Verticillium* wilt resistance (Simko et al., 2003, 2004a, 2004b).

Our study uncovered epistasis between the *StCDF1* and *Ve2* genes, where *StCDF1* functioned downstream of the *Ve2* gene. The interaction between the two genes was not direct as *Ve2* encodes a membrane protein (Kawchuk et al., 2001) and *StCDF1* functions in the nucleus as a transcriptional repressor (Kloosterman et al., 2013). *StCDF1* encoded a transcription repressor of *StCOL1/2*, which itself is an activator of *StSP5G* (Abelenda et al., 2016; Kloosterman et al., 2013). Hence, *StCDF1* also represses *StSP5G* indirectly. *StSP6A* is repressed by *StSP5G* so downregulation of the latter increases the former, which leads to tuberization. Clones homozygous for the *StCDF1.3* allele (h) had the lowest disease resistance scores. This was attributed to the loss of protein degradation for the StCDF1.3 protein (Kloosterman et al., 2013). Accumulation of StCDF1.3 under long days triggered early maturity and tuberization which was scored as low disease resistance. The presence of the *Ve2* resistance allele significantly increased disease resistance in the hh background. Clones carrying the *StCDF1.1* allele (k) had increased disease resistance, which was attributed to the production of full length protein. The full-length StCDF1.1 undergoes degradation under long days leading to delayed maturity and tuberization, which was scored as high disease resistance. Although disease resistance scores were high for clones carrying the *StCDF1.1* k allele, the *Ve2* resistance allele did not increase disease resistance. One explanation for differences in *Ve2* interaction with *StCDF1.1* and *StCDF1.3* is that the *Ve2* resistance functions through downregulation of *StCDF1*. The *StCDF1.1* (k) allele produce proteins that are already downregulated through protein degradation, therefore, effects of the *Ve2* gene would not be detected. The *StCDF1.3* (h) homozygotes express a truncated protein that is not degraded, therefore, effects of downregulation can be detected.

Clones carrying the *StCDF1* h allele from this study had lower expression of *StSP5G* compared with clones carrying the k allele. *StSP5G* expression showed increased expression in the presence of *Ve2* resistance alleles in the hh background but not in the presence of the k allele. The pattern of *StSP5G* expression in *StCDF1* and *Ve2* genotypes was similar to disease resistance and the QTL for disease resistance on chromosome 5 overlapped with the eQTL for *StSP5G*. These results suggest that the observed epistasis of *StCDF1* with *Ve2* in disease resistance involves regulation of *StSP5G* expression. The eQTL for *StSP6A* on chromosome 5 was also co-localized with disease resistance and the eQTL for *StSP5G*. The effects of the *StCDF1.3* (h) and *StCDF1.1* (k) alleles on *StSP5G* and *StSP6A* expression were opposite, which is consistent with the repression of *StSP6A* expression by *StSP5G* (Abelenda et al., 2016; Kloosterman et al., 2013; Navarro et al., 2011). However, the increased expression levels of *StSP5G* in hh*uv versus hh*uu, was not concomitant with decreased expression of *StSP6A* in hh*uv genotypes compared to hh*uu. These results suggest that *StSP5G* may regulate other downstream genes in response to the *Ve2* resistance allele in regulating the timing of maturity and tuberization. Further investigation of the molecular mechanism of the epistasis between *StCDF1* and *Ve2* will be required. Nonetheless, the current study has provided evidence for supporting a role for *StCDF1* and photoperiod-regulated tuberization pathway in *V. dahliae* resistance. The results also suggest that the *V. dahliae* pathogen activates the *StCDF1* pathway in inducing early

dying. We propose that *StCDF1* integrates multiple signals in controlling timing of tuberization in potato including photoperiod and pathogen stress.

The GO analysis of the genes with eQTL at the *Ve2* locus showed an enrichment of the GO terms "defense response to fungus, incompatible interaction" and "plant-type primary cell wall biogenesis," demonstrating a role for *Ve2* in defense against *V. dahliae*. These results concur with genetic studies on resistance to *V. dahliae* (Bae et al., 2008; Kawchuk et al., 2001; Uribe et al., 2014). On the other hand, fungal response GO terms were not found for genes with eQTL at the *StCDF1* locus indicating that *StCDF1* was not involved in defense against *V. dahliae*, and supported a role for *StCDF1* downstream of pathogen attack. The most significant GO terms for both genes with eQTL at the *Ve2* and *StCDF1* loci were associated with the chloroplast including "photosynthesis." These results were correlated with the photosynthetic decline and chlorosis observed associated with vine maturity (Wohleb et al., 2014 Ewing) and *Verticillium*-induced early dying (Bowden et al., 1990). The findings from this study further suggest that the photosynthetic decline with *V. dahliae* infection may occur through activation of the *StCDF1* maturity and tuberization pathway.

Our study also provides insights for developing strategies for selection and breeding of resistance to *V. dahliae*. The evidence provided here and in studies by others demonstrate that the *Ve2* resistance allele marker can be beneficial to selection for *Verticillium* wilt disease resistance (Bae et al., 2008; Kawchuk et al., 2001; Simko et al., 2003, 2004a, 2004b; Uribe et al., 2014). Additionally, the results suggest that selection for *StCDF1.1* can reduce symptoms of wilting, chlorosis, and early dying; however, selection for reduced symptoms alone can lead to selection of late maturation and tolerance for the pathogen. Co-selection for *V. dahliae* resistance genes, together with *StCDF1* alleles, is suggested as a strategy to reduce pathogen colonization, early dying, and development of tolerance.

Supplemental Files Available

Supplementary Fig. S1. Linkage maps for 12 potato chromosomes.

Supplementary Table S1. Tag count expression data for population 15143. The field design was a randomized complete block with three replicates plots for each clone in population 15143. The data is the LS mean over the three replicates. The LS mean for each clone was divided by LS mean for parental clone 07506–01 and the $\log_2$ ratio was used for QTL mapping.

Supplementary Table S2. Probes used in nCounter CodeSet for analysis of gene expression of *StCOL1/2* and *StSP5G* and housekeeping genes.

Supplementary Table S3. High resolution melting primer sequences. The position of the primer is forward (F), probe (P) or reverse (*R*). The Dir column indicates sense (+) or anti-sense strand (-). Chr is the chromosome, Pos is the location of the primer on the chromosome, Sequence is the 5' to 3' sequence of the primer. The potato genome sequence version was PGSC S. tuberosom group Phureja DM1–3 Pseudomolecules v.4.03.

Supplementary Table S4. Lists of genes with eQTL at *Ve2* locus.

Supplementary Table S5. Lists of genes with eQTL at *StCDF1* locus.

Supplementary Table S6. GO annotations for genes with eQTL at *StCDF1* and *Ve2* loci.

Conflict of Interest Disclosure

The authors declare that there is no conflict of interest.

Acknowledgments

The study was funded through A-base funds from Agriculture and Agri-Food Canada. Technical assistance was provided by Kraig Worrall, Cuijian Zeng, Kathryn Douglass, and Donna Wilson. Daniel Frank, Boshen Gao, Greg Conn and Woojong Rho were undergraduate students who contributed to the study. The authors would also like to thank Hielke (Henry) De Jong who established the diploid clones used in the study. Hui Ying Wang received support from the Agriculture and Agri-Food Canada–Ministry of Education (China) program.

References

Abelenda, J.A., E. Cruz-Oró, J.M. Franco-Zorrilla, and S. Prat. 2016. Potato *StCONSTANS*-like1 Suppresses Storage Organ Formation by Directly Activating the *FT*-like StSP5G Repressor. Curr. Biol. 26:872–881. doi:10.1016/j.cub.2016.01.066

Alexa, A. and J. Rahnenfuhrer. 2010. topGO: Enrichment analysis for gene ontology. R package version 2.

Bae, J., D. Halterman, and S. Jansky. 2008. Development of a molecular marker associated with *Verticillium* wilt resistance in diploid interspecific potato hybrids. Mol. Breed. 22:61–69. doi:10.1007/s11032-008-9156-8

Banerjee, A.K., M. Chatterjee, Y. Yu, S.-G. Suh, W.A. Miller, and D.J. Hannapel. 2006. Dynamics of a mobile RNA of potato involved in a long-distance signaling pathway. Plant Cell 18:3443–3457. doi:10.1105/tpc.106.042473

Beckman, C.H. 1964. Host responses to vascular infection. Annu. Rev. Phytopathol. 2:231–252. doi:10.1146/annurev.py.02.090164.001311

Bowden, R.L., D.I. Rouse, and T.D. Sharkey. 1990. Mechanism of photosynthesis decrease by *Verticillium dahliae* in Potato. Plant Physiol. 94:1048–1055. doi:10.1104/pp.94.3.1048

Chapman, H.W. 1958. Tuberization in the potato plant. Physiol. Plant. 11:215–224. doi:10.1111/j.1399-3054.1958.tb08460.x

Chen, H., F.M. Rosin, S. Prat, and D.J. Hannapel. 2003. Interacting transcription factors from the three-amino acid loop extension superclass regulate tuber formation. Plant Physiol. 132:1391–1404. doi:10.1104/pp.103.022434

Chen, X., C.A. Hackett, R.E. Niks, P.E. Hedley, C. Booth, et al. 2010. An eQTL analysis of partial resistance to *Puccinia hordei* in Barley. PLoS One 5:E8598. doi:10.1371/journal.pone.0008598

Concibido, V.C., G.A. Secor, and S.H. Jansky. 1994. Evaluation of resistance to *Verticillium* wilt in diploid, wild potato interspecific hybrids. Euphytica 76:145–152. doi:10.1007/BF00024033

Corsini, D. and J.J. Pavek. 1996. Agronomic performance of potato germplasm selected for high resistance to verticillium wilt. American potato journal. June 73:249–260. doi:10.1007/BF02849275

Corsini, D., J.J. Pavek, and J.R. Davis. 1988. Verticillium wilt resistance in noncultivated tuber-bearing *Solanum* species. Plant Dis. 72:148–151. doi:10.1094/PD-72-0148

Daayf, F. 2015. *Verticillium* wilts in crop plants: Pathogen invasion and host defence responses. Can. J. Plant Pathol. 37:8–20. doi:10.1080/07060661.2014.989908

Davies, P.J., and S. Gan. 2012. Towards an integrated view of monocarpic plant senescence. Russ. J. Plant Physiol. 59:467–478. doi:10.1134/S102144371204005X

de Almeida, M.R., D. de Bastiani, M.L. Gaeta, J.E. de Araújo Mariath, F. de Costa, J. Retallick, L. Nolan, H.H. Tai, M.V. Strömvik, and A.G. Fett-Neto. 2015. Comparative transcriptional analysis provides new insights into the molecular basis of adventitious rooting recalcitrance in Eucalyptus. Plant Sci. 239:155–165. doi:10.1016/j.plantsci.2015.07.022

De Koeyer, D., K. Douglass, A. Murphy, S. Whitney, L. Nolan, Y. Song, and W. De Jong. 2010. Application of high-resolution DNA melting for genotyping and variant scanning of diploid and autotetraploid potato. Mol. Breed. 25:67–90. doi:10.1007/s11032-009-9309-4

Diwan, N., R. Fluhr, Y. Eshed, D. Zamir, and S.D. Tanksley. 1999. Mapping of Ve in tomato: A gene conferring resistance to the broad-spectrum pathogen, *Verticillium dahliae* race 1. Theor. Applied Genet. 98:315–319. doi:10.1007/s001220051075

Druka, A., E. Potokina, Z. Luo, N. Jiang, X. Chen, M. Kearsey, and R. Waugh. 2010. Expression quantitative trait loci analysis in plants. Plant Biotechnol. J. 8:10–27. doi:10.1111/j.1467-7652.2009.00460.x

Ewing, E.E., and P.C. Struik. 1992. Tuber formation in potato: Induction, initiation, and growth. Hortic. Rev. (Am. Soc. Hortic. Sci.) 14:89.

Felcher, K.J., J.J. Coombs, A.N. Massa, C.N. Hansey, J.P. Hamilton, R.E. Veilleux, C.R. Buell, and D.S. Douches. 2012. Integration of two diploid potato linkage maps with the potato genome sequence. PLoS One 7:E36347. doi:10.1371/journal.pone.0036347

Fornara, F., K.C.S. Panigrahi, L. Gissot, N. Sauerbrunn, M. Rühl, J.A. Jarillo, and G. Coupland. 2009. Arabidopsis DOF transcription factors act redundantly to reduce CONSTANS expression and are essential for a photoperiodic flowering response. Dev. Cell 17:75–86. doi:10.1016/j.devcel.2009.06.015

Fradin, E.F., and B.P.H.J. Thomma. 2006. Physiology and molecular aspects of *Verticillium* wilt diseases caused by *V. dahliae* and *V. albo-atrum*. Mol. Plant Pathol. 7:71–86. doi:10.1111/j.1364-3703.2006.00323.x

Geiss, G.K., R.E. Bumgarner, B. Birditt, T. Dahl, N. Dowidar, et al. 2008. Direct multiplexed measurement of gene expression with color-coded probe pairs. Nat. Biotechnol. 26:317–325. doi:10.1038/nbt1385

Ghate, T.H., P. Sharma, K.R. Kondhare, D.J. Hannapel, and A.K. Banerjee. 2017. The mobile RNAs, StBEL11 and StBEL29, suppress growth of tubers in potato. Plant Mol. Biol. 93:563–578. doi:10.1007/s11103-016-0582-4

González-Schain, N.D., M. Díaz-Mendoza, M. Żurczak, and P. Suárez-López. 2012. Potato CONSTANS is involved in photoperiodic tuberization in a graft-transmissible manner. Plant J. 70:678–690. doi:10.1111/j.1365-313X.2012.04909.x

Gregory, L.E. 1956. Some factors for tuberization in the potato plant. Am. J. Bot. 43:281–288. doi:10.2307/2438945

Hannapel, D.J., P. Sharma, T. Lin, and A.K. Banerjee. 2017. The multiple signals that control tuber formation. Plant Physiol. 174:845–856. doi:10.1104/pp.17.00272

Hirsch, C.D., J.P. Hamilton, K.L. Childs, J. Cepela, E. Crisovan, B. Vaillancourt, C.N. Hirsch, M. Habermann, B. Neal, and C.R. Buell. 2014. Spud DB: A Resource for mining sequences, genotypes, and phenotypes to accelerate potato breeding. Plant Genome 7. doi:10.3835/plantgenome2013.12.0042

Holloway, B., and B. Li. 2010. Expression QTLs: Applications for crop improvement. Mol. Breed. 26:381–391. doi:10.1007/s11032-010-9396-2

Imaizumi, T., T.F. Schultz, F.G. Harmon, L.A. Ho, and S.A. Kay. 2005. FKF1 F-Box protein mediates cyclic degradation of a repressor of *CONSTANS* in *Arabidopsis*. Science 309:293–297. doi:10.1126/science.1110586

Inderbitzin, P., R.M. Bostock, R.M. Davis, T. Usami, H.W. Platt, and K.V. Subbarao. 2011. Phylogenetics and taxonomy of the fungal vascular wilt pathogen *Verticillium*, with the Descriptions of Five New Species. PLoS One 6:E28341. doi:10.1371/journal.pone.0028341

Jansky, S.H., and J.C. Miller. 2010. Evaluation of *Verticillium* wilt resistance in Russet Norkotah and six strain selections. Am. J. Potato Res. 87:492–496. doi:10.1007/s12230-010-9151-6

Jansky, S.H., and D.I. Rouse. 2000. Identification of potato interspecific hybrids resistant to *Verticillium* wilt and determination of criteria for resistance assessment. Potato Res. 43:239–251. doi:10.1007/BF02358083

Jansky, S.H., D.I. Rouse, and P.J. Kauth. 2004. Inheritance of resistance to *Verticillium dahliae* in diploid interspecific potato hybrids. Plant Dis. 88:1075–1078. doi:10.1094/PDIS.2004.88.10.1075

Johnson, D.A., and J.K.S. Dung. 2010. *Verticillium* wilt of potato—The pathogen, disease, and management. Can. J. Plant Pathol. 32:58–67. doi:10.1080/07060661003621134

Kawchuk, L.M., J. Hachey, D.R. Lynch, F. Kulcsar, G. van Rooijen et al. 2001. Tomato Ve disease resistance genes encode cell surface-like receptors. Proc. Natl. Acad. Sci. USA 98:6511–6515. doi:10.1073/pnas.091114198

Kloosterman, B., J.A. Abelenda, M.M.C. Gomez, M. Oortwijn, J.M. de Boer, et al. 2013. Naturally occurring allele diversity allows potato cultivation in northern latitudes. Nature 495:246–250. doi:10.1038/nature11912

Kloosterman, B., A. Anithakumari, P.-Y. Chibon, M. Oortwijn, G.C. van der Linden, R.G. Visser, and C.W. Bachem. 2012. Organ specificity and transcriptional control of metabolic routes revealed by expression QTL profiling of source-sink tissues in a segregating potato population. BMC Plant Biol. 12:17. doi:10.1186/1471-2229-12-17

Korves, T.M., and J. Bergelson. 2003. A developmental response to pathogen infection in *Arabidopsis*. Plant Physiol. 133:339–347. doi:10.1104/pp.103.027094

Li, X.-Q., D. Sveshnikov, B. Zebarth, H. Tai, D. De Koeyer, P. Millard, M. Haroon, and M. Singh. 2010. Detection of nitrogen sufficiency in potato plants using gene expression markers. Am. J. Potato Res. 87:50–59. doi:10.1007/s12230-009-9116-9

Luo, S., H. Tai, B. Zebarth, X.-Q. Li, P. Millard, D. De Koeyer, and X. Xiong. 2011. Sample collection protocol effects on quantification of gene expression in potato leaf tissue. Plant Mol. Biol. Report. 29:369–378. doi:10.1007/s11105-010-0239-4

Lynch, D.R., L.M. Kawchuk, J. Hachey, P.S. Bains, and R.J. Howard. 1997. Identification of a gene conferring high levels of resistance to *Verticillium* wilt in *Solanum chacoense*. Plant Dis. 81:1011–1014. doi:10.1094/PDIS.1997.81.9.1011

Lyons, R., A. Rusu, J. Stiller, J. Powell, J.M. Manners, and K. Kazan. 2015. Investigating the association between flowering time and defense in the *Arabidopsis thaliana–Fusarium oxysporum* Interaction. PLoS One 10:E0127699. doi:10.1371/journal.pone.0127699

Martínez-García, J.F., A. Virgós-Soler, and S. Prat. 2002. Control of photoperiod-regulated tuberization in potato by the Arabidopsis flowering-time gene CONSTANS. Proc. Natl. Acad. Sci. USA 99:15,211–15,216. doi:10.1073/pnas.222390599

Mézard, C. 2006. Meiotic recombination hotspots in plants. Biochem. Soc. Trans. 34:531–534. doi:10.1042/BST0340531

Morris, W.L., R.D. Hancock, L.J.M. Ducreux, J.A. Morris, M. Usman, S.R. Verrall, S.K. Sharma, G. Bryan, J.W. McNicol, P.E. Hedley, and M.A. Taylor. 2014. Day length dependent restructuring of the leaf transcriptome and metabolome in potato genotypes with contrasting tuberization phenotypes. Plant Cell Environ. 37:1351–1363. doi:10.1111/pce.12238

Nakane, E., K. Kawakita, N. Doke, and H. Yoshioka. 2003. Elicitation of primary and secondary metabolism during defense in the potato. J. Gen. Plant Pathol. 69:378–384. doi:10.1007/s10327-003-0075-6

Navarro, C., J.A. Abelenda, E. Cruz-Oro, C.A. Cuellar, S. Tamaki, J. Silva, K. Shimamoto, and S. Prat. 2011. Control of flowering and storage organ formation in potato by FLOWERING LOCUS T. Nature 478:119–122. doi:10.1038/nature10431

Nicot, N., J.-F. Hausman, L. Hoffmann, and D. Evers. 2005. Housekeeping gene selection for real-time RT-PCR normalization in potato during biotic and abiotic stress. J. Exp. Bot. 56:2907–2914. doi:10.1093/jxb/eri285

Nielsen, K.L., A.L. Høgh, and J. Emmersen. 2006. DeepSAGE—Digital transcriptomics with high sensitivity, simple experimental protocol and multiplexing of samples. Nucleic Acids Res. 34:e133. doi:10.1093/nar/gkl714

Pegg, G.F., and B.L. Brady. 2002. *Verticillium* wilts. CAB International, London. doi:10.1079/9780851995298.0000

Pin, P.A., and O. Nilsson. 2012. The multifaceted roles of FLOWERING LOCUS T in plant development. Plant Cell Environ. 35:1742–1755. doi:10.1111/j.1365-3040.2012.02558.x

Quinones, V., S. Zanlungo, L. Holuigue, S. Litvak, and X. Jordana. 1995. The cox1 initiation codon is created by RNA editing in potato mitochondria. Plant Physiol. 108:1327–1328. doi:10.1104/pp.108.3.1327

Ranjan, A., J.M. Budke, S.D. Rowland, D.H. Chitwood, R. Kumar, L. Carriedo, Y. Ichihashi, K. Zumstein, J.N. Maloof, and N.R. Sinha.

2016. eQTL regulating transcript levels associated with diverse biological processes in tomato. Plant Physiol. 172:328–340. doi:10.1104/pp.16.00289

R Core Team. 2016. R: A language and environment for statistical computing. R Foundation for Statistical Computing, Vienna, Austria. https://www.R-project.org/

Robinson, M.D., D.J. McCarthy, and G.K. Smyth. 2010. edgeR: A bioconductor package for differential expression analysis of digital gene expression data. Bioinformatics 26:139–140. doi:10.1093/bioinformatics/btp616

Rodriguez-Falcon, M., J. Bou, and S. Prat. 2006. Seasonal control of tuberization in potato: Conserved elements with the flowering response. Annu. Rev. Plant Biol. 57:151–180. doi:10.1146/annurev.arplant.57.032905.105224

Rowe, R.C. and M.L. Powelson. 2002. Potato early dying: Management challenges in a changing production environment. Plant disease. Nov 86:1184–1193.

Sawa, M., D.A. Nusinow, S.A. Kay, and T. Imaizumi. 2007. FKF1 and GIGANTEA complex formation is required for day-length measurement in *Arabidopsis*. Science 318(5848):261–265. doi:10.1126/science.1146994

Sharma, P., T. Lin, and D.J. Hannapel. 2016. Targets of the *StBEL5* transcription factor include the FT ortholog *StSP6A*. Plant Physiol. 170(1):310–324. doi:10.1104/pp.15.01314

Sharma, S.K., D. Bolser, J. de Boer, M. Sønderkær, W. Amoros, et al. 2013. Construction of reference chromosome-scale pseudomolecules for potato: Integrating the potato genome with genetic and physical maps. G3: Genes, Genomes, Genet. 3(11):2031–2047. doi:10.1534/g3.113.007153

Shim, J.S., A. Kubota, and T. Imaizumi. 2017. Circadian clock and photoperiodic flowering in *Arabidopsis*: CONSTANS is a hub for signal integration. Plant Physiol. 173:5–15. doi:10.1104/pp.16.01327

Simko, I., S. Costanzo, K. Haynes, B. Christ, and R. Jones. 2003. Identification of molecular markers linked to the *Verticillium* wilt resistance gene homologue in potato (*Solanum tuberosum* L.). Acta Hortic. 619:127–133. doi:10.17660/ActaHortic.2003.619.13

Simko, I., S. Costanzo, K.G. Haynes, B.J. Christ, and R.W. Jones. 2004a. Linkage disequilibrium mapping of a *Verticillium dahliae* resistance quantitative trait locus in tetraploid potato (*Solanum tuberosum*) through a candidate gene approach. Theor. Appl. Genet. 108:217–224. doi:10.1007/s00122-003-1431-9

Simko, I., and K.G. Haynes. 2016. Maturity-adjusted resistance of potato (*Solanum tuberosum* L.) cultivars to *Verticillium* wilt caused by *Verticillium dahliae*. Am. J. Potato Res. 94(2):173–177. doi:10.1007/s12230-016-9553-1

Simko, I., K.G. Haynes, E.E. Ewing, S. Costanzo, B.J. Christ, and R.W. Jones. 2004b. Mapping genes for resistance to *Verticillium albo-atrum* in tetraploid and diploid potato populations using haplotype association tests and genetic linkage analysis. Mol. Genet. Genomics 271:522–531. doi:10.1007/s00438-004-1010-z

Simko, I., K.G. Haynes, and R.W. Jones. 2004c. Mining data from potato pedigrees: Tracking the origin of susceptibility and resistance to *Verticillium dahliae* in North American cultivars through molecular marker analysis. Theor. Appl. Genet. 108:225–230. doi:10.1007/s00122-003-1448-0

Sliwka, J., H. Jakuczun, M. Chmielarz, A. Hara-Skrzypiec, I. Tomczynska, A. Kilian, and E. Zimnoch-Guzowska. 2012. A resistance gene against potato late blight originating from *Solanum* × *michoacanum* maps to potato chromosome VII. Theor. Appl. Genet. 124:397–406. doi:10.1007/s00122-011-1715-4

Su, Z., X. Ma, H. Guo, N.L. Sukiran, B. Guo, S.M. Assmann, and H. Ma. 2013. Flower development under drought stress: Morphological and transcriptomic analyses reveal acute responses and long-term acclimation in Arabidopsis. Plant Cell 25:3785–3807. doi:10.1105/tpc.113.115428

Supek, F., M. Bošnjak, N. Škunca, and T. Šmuc. 2011. REVIGO summarizes and visualizes long lists of gene ontology terms. PLoS One 6:E21800. doi:10.1371/journal.pone.0021800

Tai, H., G. Conn, C. Davidson, and H. Platt. 2009. Arbitrary multi-gene reference for normalization of real-time PCR gene expression data. Plant Mol. Biol. Report. 27:315–320. doi:10.1007/s11105-009-0089-0

Tai, H.H., C. Goyer, H.W. Platt, D. De Koeyer, A. Murphy, P. Uribe, and D. Halterman. 2013. Decreased defense gene expression in tolerance versus resistance to *Verticillium dahliae* in potato. Funct. Integr. Genomics 13:367–378. doi:10.1007/s10142-013-0329-0

Talboys, P.W. 1972. Resistance to vascular wilt fungi. Proc. R. Soc. Lond. B Biol. Sci. 181:319–332. doi:10.1098/rspb.1972.0053

Thomas, H. 2013. Senescence, ageing and death of the whole plant. New Phytol. 197:696–711. doi:10.1111/nph.12047

Turck, F., F. Fornara, and G. Coupland. 2008. Regulation and identity of florigen: FLOWERING LOCUS T moves center stage. Annu. Rev. Plant Biol. 59:573–594. doi:10.1146/annurev.arplant.59.032607.092755

Uribe, P., S. Jansky, and D. Halterman. 2014. Two CAPS markers predict *Verticillium* wilt resistance in wild *Solanum* species. Mol. Breed. 33:465–476. doi:10.1007/s11032-013-9965-2

Wan, C.Y., and T.A. Wilkins. 1994. A modified hot borate method significantly enhances the yield of high-quality RNA from cotton (*Gossypium hirsutum* L.). Anal. Biochem. 223:7–12. doi:10.1006/abio.1994.1538

Wang, G.-F., S. Seabolt, S. Hamdoun, G. Ng, J. Park, and H. Lu. 2011. Multiple roles of WIN3 in regulating disease resistance, cell death, and flowering time in *Arabidopsis*. Plant Physiol. 156:1508–1519. doi:10.1104/pp.111.176776

Wenzl, P., J. Carling, D. Kudrna, D. Jaccoud, E. Huttner, A. Kleinhofs, and A. Kilian. 2004. Diversity Arrays Technology (DArT) for whole-genome profiling of barley. Proc. Natl. Acad. Sci. USA 101:9915–9920. doi:10.1073/pnas.0401076101

Wohleb, C.H., R.N. Knowles, and M.J. Pavek. 2014. Plant growth and development. In: R. Navarre and M.J. Pavek, editors, The potato: Botany, production and uses. CABI, Boston, MA. p. 64–82.

Yadeta, K., and B. Thomma. 2013. The xylem as battleground for plant hosts and vascular wilt pathogens. Front. Plant Sci. 4. doi:10.3389/fpls.2013.00097

Zhang, F., E. Boerwinkle, and M. Xiong. 2014. Epistasis analysis for quantitative traits by functional regression model. Genome Res. 24:989–998. doi:10.1101/gr.161760.113